Available online at www.sciencedirect.com
ScienceDirect
Mendeleev Commun., 2013, **23**, 101–103

Mendeleev Communications

Mass spectra of 3-substituted 2-oxosparteines

Anna K. Przybył* and Zdzisława Nowakowska

Faculty of Chemistry, A. Mickiewicz University, 61-614 Poznań, Poland. Fax: +48 61 829 6761;
e-mail: annaprz@amu.edu.pl

DOI: 10.1016/j.mencom.2013.03.017

The following sparteine derivatives obtained by the chemical modification of the lupin alkaloid 2-oxosparteine (lupanine) have been studied by EI and ESI mass spectrometry: 3-dehydrolupanine, 2-thiono-3-dehydrolupanine, 3β-phenylthiolupanine, 3α-phenylthiolupanine and 3,3-di(phenylthio)lupanine.

Sparteine and its derivatives (the modified bisquinolizidine alkaloids) are of great interest because of their chemical and biological importance.[1–7] Chemical modifications can strongly influence the potential biological activity of these compounds; thus, the knowledge of their molecular structures and decomposition pathways is of great importance. The recent interest in quinolizidine alkaloids has prompted the search for spectroscopic methods that would differentiate their stereoisomers and position isomers, including mass spectrometric (MS) methods.[5–12] Here, we present the results of an EI and ESI MS study of 3-dehydrolupanine (**1**), 2-thiono-3-dehydrolupanine (**2**), 3β-phenylthiolupanine (ax, **3**), 3α-phenylthiolupanine (eq, **4**) and 3,3-di(phenylthio)lupanine (**5**) (Figure 1). Compounds **1**–**5** were synthesized and characterized by NMR and X-ray methods.[13,14] The standard EI mass spectra (70 eV) of **1**–**5**, the relative abundances and elemental compositions of characteristic ions, and the pathways of the EI mass fragmentation of the compounds studied are given in Scheme 1 and Table 1. The characteristic features of the mass fragmentation of the molecular ion of compound **1** are bond cleavages in rings B and C. In the GC-MS spectrum of **1** apart from the molecular ion **a** with *m/z* 246, there are also very abundant $[M-{}^{\bullet}H]^+$ ion **b** as well as ions **e** and **g** [Table 1, Figure 2(*a*)].

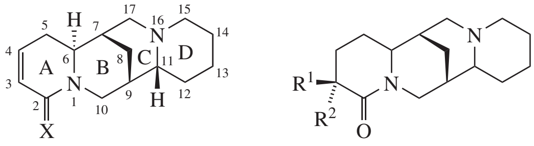

1 X = O
2 X = S

3 R^1 = SPh, R^2 = H
4 R^1 = H, R^2 = SPh
5 R^1 = R^2 = SPh

Figure 1 Structures of compounds **1**–**5**.

The simple cleavages of C_{sp^3}–C_{sp^3} and C_{sp^3}–N bonds (C^6–C^7, C^{10}–N^1) of ring B gave the even-electron ion **e** at *m/z* 150. The formation of this ion requires a rearrangement of two hydrogen atoms. In the next step of fragmentation, the elimination of an H_2 molecule gives ion **f** at *m/z* 148, which is the parent ion of even-electron fragment ion **i** (*m/z* 122, B^2/E linked scan spectra), obtained by :C=CH_2 elimination (Scheme 1). The next abundant product, *i.e.* even-electron fragment ion **g** at *m/z* 136 derived from $M^{+\bullet}$ ion **a**, is formed by the cleavages of C^6–C^7 and C^9–C^{10} bonds in ring B. Based on B^2/E mass spectra of **1** and **2**, ion **g** can also be obtained from ion **e** (*m/z* 150) by the elimination of :CH_2. In the next step, the loss of H_2 or :CH_2 by ion **g** takes place and ions **h** (*m/z* 134) and **i** (m/z 122), respectively, are obtained (Scheme 1). The principal mass fragmentation of the molecular ion **a** of **2** is similar in some respects to the fragmentations of oxo analogue **1**, but show differences in the abundances of some fragment ions (Scheme 1, Table 1). The molecular ion of **1** is less abundant than that of compound **2** (Figure 2). This suggests that the presence of a sulfur atom has no influence on the main routes of its mass fragmentation but increases the stability of molecular ion. $[M-{}^{\bullet}H]^+$ ion **b** of **2** is the base peak in the GC-MS spectra, whereas ion **b** of **1** has 65% of relative abundance (Table 1). The analysis of the mass spectra of **1** and **2** revealed the appearance of a peak at *m/z* 229 for compound **2** as a result of the elimination of an ${}^{\bullet}$SH radical, while the elimination of an ${}^{\bullet}$OH radical from ion **a** of **1** was not observed (Figure 2). The molecular ion of **2** can also decompose by the loss of the CH_2=C=S molecule to give an ion with *m/z* 204. This fragmentation step occurs *via* a hydrogen rearrangement followed by C^3–C^4 and C^2–N bond cleavages, but the elimination of the CH_2=C=O fragment was not observed for the molecular ion **a** of **1**.

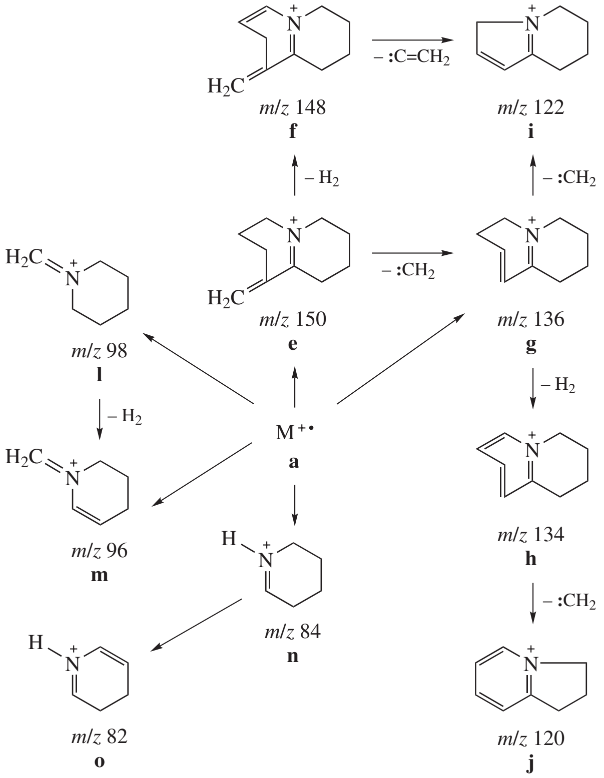

Scheme 1 Fragmentation pathways in the spectra of compounds **1**–**5**.

Differences in the relative abundances of molecular ions and even-electron ion **b** $[M-{}^{\bullet}H]^+$, as well as ions **e** (*m/z* 150),

Table 1 Relative abundance of characteristic ions in the EI-MS spectra of compounds **1**–**5**.

Ion	Elemental composition	*m*/*z*	Relative abundance (%)				
			1	**2**	**3** ax	**4** eq	**5**
M$^{+\bullet}$	$C_{15}H_{22}N_2O$	246	32	–	–	–	–
a	$C_{15}H_{22}N_2S$	262	–	55	–	–	–
	$C_{21}H_{28}N_2OS$	356	–	–	0	0	–
	$C_{27}H_{32}N_2OS_2$	464	–	–	–	–	7
[M–$^{\bullet}$H]$^+$	$C_{15}H_{21}N_2O$	245	65	–	–	–	–
b	$C_{15}H_{21}N_2S$	261	–	100	–	–	–
	$C_{21}H_{27}N_2OS$	355	–	–	0	1	–
	$C_{27}H_{31}N_2OS_2$	463	–	–	–	–	–
[M–$^{\bullet}$SPh]$^+$	$C_{21}H_{27}N_2OS$	355	–	–	–	–	100
c	$C_{15}H_{23}N_2O$	247	–	–	100	100	–
[M–$^{\bullet}$XH]$^+$	$C_{15}H_{21}N_2$	229	–	64	–	–	–
d	$C_{21}H_{27}N_2S$	339	–	–	–	2	–
	$C_{27}H_{31}N_2OS$	431	–	–		–	–
e	$C_{10}H_{16}N$	150	69	27	4	2	5
f	$C_{10}H_{14}N$	148	49	57	76	82	15
g	$C_9H_{14}N$	136	100	60	12	9	6
h	$C_9H_{12}N$	134	54	80	17	18	9
i	$C_8H_{12}N$	122	27	20	3	3	3
j	$C_8H_{10}N$	120	14	10	3	5	3
k	$C_7H_{12}N$	110	46	9	9	8	8
l	$C_6H_{12}N$	98	27	19	17	13	8
m	$C_6H_{10}N$	96	24	18	4	5	6
n	$C_5H_{10}N$	84	33	14	7	6	17
o	C_5H_8N	82	26	10	6	5	5

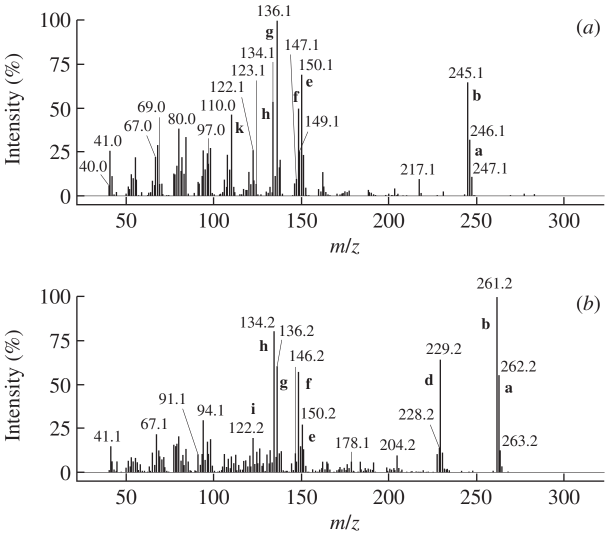

Figure 2 Low-resolution EI mass spectra obtained for compounds (*a*) **1** and (*b*) **2**.

g (*m*/*z* 136) and **k** (*m*/*z* 110) (Table 1), in the mass spectra of **1** and **2** depend clearly on the presence of a sulfur atom in the molecule. The introduction of an SPh substituent into ring A in the C-3 position decreased the relative abundance of the molecular ion **a** and [M–$^{\bullet}$H]$^+$ ion **b**. The loss of the $^{\bullet}$SPh radical is the dominant fragmentation path for **3** and **4**. As a result of this decomposition, ion **c** (*m*/*z* 247) manifested itself. Other abundant ions **f**, **h** and **l** were observed by cleavages of the C_{sp^3}–C_{sp^3} bonds of ring B or C. It is possible to distinguish two isomers **3** and **4** based on the EI and ESI mass spectra assuming their retention times[5,†] on GC-MS, which are 24.227 min for **3** and 24.359 min for **4**. For **5**, the most abundant ion **c** is that formed by the elimination of the $^{\bullet}$SPh radical from molecular ion **a** (*m*/*z* 355, Table 1).

Although, electrospray ionization (ESI) is a mild ionization method, it is well known that, by varying potential differences between the sampling cone and the skimmer in the ESI ion source, the collision-induced dissociation (CID) of these ions occurs. The production of these structurally characteristic fragments at a high cone voltage (cv) can be very helpful for the identification of alkaloids.

We analyzed in more detail the mass spectrometric fragmentation pathways of protonated sparteine derivatives **1**–**5**.[‡] When the ESI mass spectrometry experiments were carried out in the positive mode and the ESI MS of **1** at cv of 30–70 V, the protonated molecular ion [M+H]$^+$ at *m*/*z* 247 as a base peak was observed, while low-abundant fragment ions at *m*/*z* 112, 134, 136, 148 and 150 were seen in a range of 50–90 V in addition to the dominant protonated molecule. The relative abundance of fragment ions increases with cone voltage. At cv of 90 V, the fragment ion at *m*/*z* 136 [$C_9H_{14}N$]$^+$ is the base peak in the spectrum. The ESI MS of **3** recorded at cv of 30 V showed only the [M+H]$^+$ ion at *m*/*z* 357. With growing cone voltage, the fragmentation of the [M+H]$^+$ ion of compound **3** proceeded. Three peaks observed at *m*/*z* 247, 148 and 136 can be assigned to the ions [M–$^{\bullet}$SPh]$^+$, [$C_{10}H_{14}N$]$^+$ and [$C_9H_{14}N$]$^+$, respectively. For cv of 70 and 90 V, the ion at *m*/*z* 136 was the base peak. When **4** was subjected to collision-induced dissociation at a collision energy of 30 eV, it yielded abundant ions at *m*/*z* 357, 355, 247 and 245 identified as [M+H]$^+$, [M+H–H_2]$^+$, [M–$^{\bullet}$SPh]$^+$ and [M–H_2–$^{\bullet}$SPh]$^+$ ions, respectively. With increasing cv to 50–90 V, a decrease in the abundance of the former ions and an increase in the abundance of ions [$C_9H_{14}N$]$^+$ (**g**, *m*/*z* 136) and [$C_{10}H_{14}N$]$^+$ (**f**, *m*/*z* 148, base peak) were observed. In the ESI MS of **5** at cv of 30 and 50 V, [M+H]$^+$ (*m*/*z* 465, base peak) and [M+H–H_2]$^+$ ions (*m*/*z* 463), as well as the [M+H–$^{\bullet}$SPh]$^{+\bullet}$ ion (*m*/*z* 356), manifested themselves (Figure 3). An increase in cv to 70 V or higher caused the decomposition of the second $^{\bullet}$SPh fragment (*m*/*z* 247). For cv of 50–90 V, the ion at *m*/*z* 323 derived from the [M+H–$^{\bullet}$SPh]$^{+\bullet}$ parent ion by the loss of mass 33 was formed; thus, the elimination of $^{\bullet}$SH took place. At cv of 70 and 90 V, ions **h** (*m*/*z* 134), **g** (*m*/*z* 136), **f** (*m*/*z* 148) and **e** (*m*/*z* 150) with high abundance were also formed.

In conclusion, the fragmentation of molecular ion **2** leads to the elimination of the $^{\bullet}$SH radical, while the elimination of the $^{\bullet}$OH radical from ion **a** was not observed for compound **1**. For the molecular ions of **3**–**5**, the dominant fragmentation path is the loss of the $^{\bullet}$SPh radical. The retention time (GC-MS) is helpful

---

[†] GC-MS analyses were performed on a CP3800 gas chromatograph associated with a mass spectrometer (4000MS, ion trap). The column was VF-5ms 30 m×0.25 mm×0.39 mm (Varian Part no. CP8944); the carrier gas was helium with a flow rate of 1 ml min^{-1}. Injector type 1177, std. on column, temp. 250 °C. Temperature program during GC-MS analysis: 80 °C/1 °C/1 min; 180 °C/20 °C/1 min/280 °C/10 °C/1 min, hold 20 min. Mass spectra were detected on a 4000MS detector (temperature trap 220 °C) in a range of *m*/*z* 40–600. Ionization mode was internal EI (energy of electrons 70 eV); sample volume, 1 or 5 μl; solvent, MeOH.

The B^2/E linked-scan spectra were recorded using an AMD Intectra GmbH (Harpsted, Germany) model 402 two-sector mass spectrometer (ionizing voltage, 70 eV; resolution, 1000 for low-resolution and 10000 for high-resolution mass spectra). These spectra were measured in the first field-free region using helium as the collision gas at a pressure of 1.73×10^{-5} mbar, ionization energy of 70 eV, and an accelerating voltage of 8 kV.

[‡] The ESI MS of compounds **1**–**5** were recorded on a ZQ mass spectrometer (Waters/Micromass, Manchester, UK) equipped with a Harvard Apparatus syringe pump. The sample solutions were prepared in methanol in a concentration 5×10^{-5} mol dm^{-3}, which is typical of ESI. The samples were infused into the ESI source using a Harvard multipump at a flow rate of 40 ml min^{-1}. The ESI source potential was 3 kV on the capillary, 0.5 kV on the lens, 4 V on the extractor, and the cone voltage was from 30 to 90 V. The source and desolvation temperatures were 120 and 300 °C, respectively. Nitrogen was used as a neutralizing and desolvation gas at flow rates of 100 and 300 dm^3 h^{-1}, respectively.

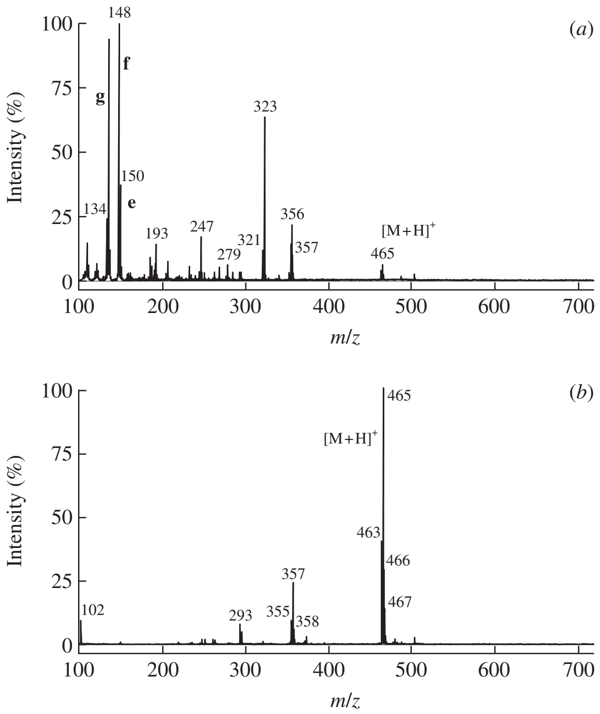

Figure 3 ESI mass spectrum of compound **5** recorded at cv of (*a*) 90 (scan ES+, 2.02×10^{8}) and (*b*) 30 V (scan ES+, 6.68×10^{7}).

for the identification of isomers **3** and **4**. Based on the low-resolution mass spectra, we can easily establish the structure of 2-oxosparteine derivatives.

References

1 A. R. Germain, D. M. Bruggemeyer, J. Zhu, C. Genet, P. O'Brien and J. A. Porco, *J. Org. Chem.*, 2011, **76**, 2577.
2 S. Priyadarshini, P. J. A. Joseph, P. Srinivas, H. Maheswaran, M. L. Kantam and S. Bhargava, *Tetrahedron Lett.*, 2011, **52**, 1615.
3 G. Barker, P. O'Brien and K. R. Campos, *ARKIVOC*, 2011, **v**, 217.
4 D. C. Ebner, R. M. Trend, C. Genet, M. J. McGrath, P. O'Brien and B. M. Stoltz, *Angew. Chem. Int. Ed.*, 2008, **47**, 6367.
5 P. M. Garcia Lopez, P. Garzon de la Mora, W. Wysocka, B. Maiztegui, M. E. Alzugaray, H. Del Zotto and M. I. Borelli, *Eur. J. Pharmacol.*, 2004, **504**, 139.
6 I. Murakoshi, Y. Fujii, S. Takeda and I. Arai, *Jap. Patent* JP04295480, 1991 (*Chem. Abstr.*, 1993, **118**, 45733).
7 M. D. Antoun and O. M. A. Taha, *J. Nat. Prod.*, 1981, **44**, 179.
8 A. K. Przybył and Z. Nowakowska, *Rapid Commun. Mass Spectrom.*, 2011, **25**, 1193.
9 A. K. Przybył and W. Prukała, *Rapid Commun. Mass Spectrom.*, 2008, **22**, 261.
10 N. S. Vulfson, Z. S. Ziyavidinova and V. G. Zaikin, *Khim. Geterotsikl. Soedin.*, 1974, 251 (in Russian).
11 R. Kolanoś and W. Wysocka, *J. Mass Spectrom.*, 2003, **38**, 343.
12 B. Jasiewicz and E. Wyrzykiewicz, *Spectrosc. Lett.*, 2009, **42**, 49.
13 A. K. Przybył and M. Kubicki, *Tetrahedron*, 2009, **65**, 3454.
14 A. K. Przybył and M. Kubicki, *Tetrahedron*, 2011, **67**, 7787.

Received: 22nd November 2012; Com. 12/4022